Mutation of a Strictly Conserved, Active-Site Residue Alters Substrate Specificity and Cofactor Biogenesis in a Copper Amine Oxidase†

Joan M. Hevel,‡ Stephen A. Mills, and Judith P. Klinman*

Department of Chemistry and Department of Molecular and Cell Biology, University of California, Berkeley, California 94720

Received September 11, 1998; Revised Manuscript Received December 28, 1998

ABSTRACT: The copper amine oxidases (CAOs) catalyze both the single-turnover modification of a peptidyl tyrosine to form the active-site cofactor 2,4,5-trihydroxyphenylalanine quinone (TPQ) and the oxidative deamination of primary amines using TPQ. The function of a strictly conserved tyrosine located within hydrogen-bonding distance to TPQ has been explored by employing site-directed mutagenesis on the enzyme from *H. polymorpha* to form the mutants Y305A, Y305C, and Y305F. Both Y305A and Y305C behave similarly with regard to aliphatic amine oxidase activity, showing 3−7-fold decreases in kinetic parameters relative to WT, while the more conservative substitution of Y305F results in a >100-fold decrease in k_{cat} and >500-fold decrease in k_{cat}/K_m relative to WT for the reductive half-reaction. The oxidation of benzylamine by all three mutants is severely impaired, with very significant effects seen in the oxidative half-reaction. CAO activity was studied as a function of pH for WT and Y305A proteins. Profiles for WT-catalyzed methylamine oxidation and Y305A-catalyzed ethylamine oxidation are comparable, while profiles of Y305A-catalyzed methylamine oxidation suggest the pH-dependent build-up of an inhibitory intermediate, which was subsequently observed spectrophotometrically and is attributed to the product Schiff base. The relative effects of mutations at Y305 on catalytic turnover are, thus, concluded to be dependent on the nature of the amino acid which substitutes for tyrosine and the substrate used in amine oxidase assays. TPQ biogenesis experiments demonstrate a ∼800-fold decrease in k_{obs} for apo-Y305A compared to WT. Despite the strict conservation of Tyr305 in all CAOs, neither biogenesis nor catalytic turnover is abolished upon mutation of this residue. We propose an important, but nonessential, role for Tyr305 in the positioning of the TPQ precursor for biogenesis, and in the maintenance of the correct conformation for TPQ-derived intermediates during catalytic turnover.

The TPQ-dependent[1] copper amine oxidases (CAOs) are a ubiquitous family of proteins which catalyze two different reactions. The precursor protein[2] is responsible for a copper-dependent, single-turnover event which converts a specific tyrosyl residue of the amine oxidase into TPQ and thus forms the mature enzyme (*2*) (Scheme 1). This copper- and TPQ-containing enzyme is, then, able to oxidatively deaminate primary amines in a traditional enzymatic fashion with multiple turnovers (*3*). Crystal structures of both apo-precursor and copper-containing mature proteins are almost superimposable with the exception of the expected small movements in the precursor tyrosine residue and the residues which bind copper (*4*). A collection of studies has shown

Scheme 1: Overall TPQ Biogenesis Reaction

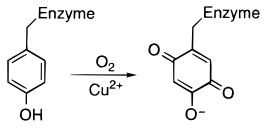

that the biogenesis of TPQ requires molecular oxygen and copper (*5*). These components, in the absence of other factors, including reducing equivalents, are sufficient for the conversion of tyrosine to TPQ *in vitro* (*6*). Mechanisms involving a copper hydroperoxide (*7*) or tyrosyl radical (*8*) have been put forth; however, neither mechanism has been supported by experimental evidence nor is there a clear understanding as to which residues may be critical for biogenesis to occur.

On the other hand, the mechanism by which the mature CAO catalyzes the 2-electron deamination of primary amines has been well documented (*9*). The ping-pong reaction of the amine oxidases can be divided into reductive and oxidative half-reactions:

$$\text{reductive half-reaction: } E_{ox} + RCH_2NH_2 \rightarrow E_{red} + RCHO \quad (1)$$

$$\text{oxidative half-reaction: } E_{red} + O_2 + H_2O \rightarrow E_{ox} + H_2O_2 + NH_3 \quad (2)$$

The reductive half-reaction (Scheme 2) begins with the

† This work was supported by a National Institutes of Health Grant (GM39296) to J.P.K. J.M.H. was supported by a National Institutes of Health Postdoctoral Fellowship (GM16143).

* To whom correspondence should be addressed.

‡ Current address: Department of Chemistry, University of Hawaii at Manoa, 2545 The Mall, Honolulu, HI 96822.

[1] Abbreviations: WT, wild type; TOPA, 2,4,6-trihydroxyphenylalanine; TPQ, TOPA quinone; ICP, inductively coupled plasma; HEPES, *N*-(2-hydroxyethyl)piperazine-*N*′-2-ethanesulfonic acid; CAO, copper amine oxidase; HPAO, yeast amine oxidase from *Hansenula polymorpha*; BSAO, bovine serum amine oxidase.

[2] The term precursor protein is defined as an amine oxidase in which the specific active-site tyrosine has not been posttranslationally modified. The term apo-precursor is defined as wild-type or mutated precursor protein that does not have copper bound at the active site. Mature protein refers to amine oxidase that has both TPQ and bound copper at the active site.

10.1021/bi982199m CCC: $18.00
Published on Web 03/05/1999

Scheme 2: Reductive Half-Reaction of Methylamine Oxidation by CAO

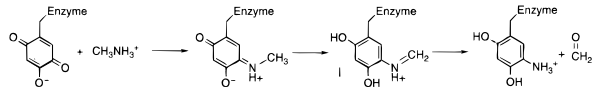

Scheme 3: Oxidative Half-Reaction of CAO

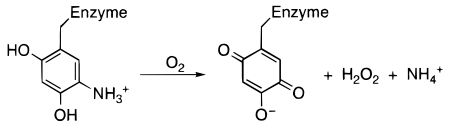

formation of a Schiff base between the amine substrate and TPQ (the substrate Schiff base), followed by proton abstraction by an active-site base to form the product Schiff base and reduced cofactor, and ends with the hydrolysis of imine to form product aldehyde and the aminoquinol form of the cofactor. The reoxidation of the cofactor by molecular oxygen (Scheme 3) is less well understood, but has been the subject of several studies using CAOs from pea seedling (*10*), lentil seedling (*11*), and bovine plasma (*12*).

While the majority of the available mechanistic studies of CAOs have been conducted with BSAO, a suitable expression system for this enzyme has not yet been developed. In light of the ease of expression and mutagenesis of a CAO from *Hansenula polymorpha*[3] (HPAO) in both *S. cerevisiae* and *E. coli* (*3*, *6*), a kinetic characterization of the HPAO is presented herein to be used as a baseline for comparison of mutant forms of this enzyme.

Crystal structures have been determined for the mature form of CAOs from *E. coli* (*13*), pea seedling amine oxidase (*14*), *Arthrobactor globiformis* (*4*), and *H. polymorpha* (*15*). Thus far, only the *H. polymorpha* structure shows the cofactor in a productive conformation,[4] revealing the proposed active-site base (Asp319) to be linked via a series of hydrogen bonds to the axial water of the cupric ion on the opposite side of the cofactor. A key residue in this hydrogen-bonded network is Tyr305, a strictly conserved residue which is within hydrogen-bonding distance of the C-4 oxygen of TPQ (*15*). With the exception of an asparagine residue which appears to be critical in the orientation of the TPQ ring (*16*), Tyr305 is the only residue within 3 Å of TPQ (*15*).

Given the position of Tyr305, we reasoned that it would play a key role in the biogenesis and/or catalytic processes of the CAOs. Proposed mechanisms for the biogenesis of TPQ involve the addition of molecular oxygen, followed by water, to the precursor Tyr405 (*6*), which could be catalyzed by Tyr305. With regard to catalytic turnover, Tyr305 is positioned as a conduit of protons from the region of the active site catalyzing substrate oxidation to the region responsible for dioxygen reduction, as well as an "anchor" for maintaining the cofactor in a non-copper-liganding orientation. As we now show, mutations at position 305 result in many unexpected properties, which include a greater reduction in the catalytic rate from the substitution of Phe compared to Ala, as well as a change in substrate specificity in favor of aliphatic amines larger than methylamine. A preliminary study of biogenesis suggests that Tyr305 may be more critical for TPQ formation than ethylamine oxidation. These effects are discussed in the context of the available structural information for the CAOs.

EXPERIMENTAL PROCEDURES

Materials and General Methods. CH_3NH_2·HCl and CD_3NH_2·HCl were purchased from Aldrich. Ethylamine hydrochloride was purchased from Fluka. Phenethylamine hydrochloride and V8 protease (type XVII-B from *Staphylococcus aureus* strain V8, 830 units/mg solid) were purchased from Sigma. Benzylamine hydrochloride was purchased from Sigma and recrystallized. [1,1-^{2}H]Benzylamine was synthesized as previously described by Hartmann and Klinman (*17*). Protein concentration was determined by the Bradford Protein assay or Micro Bradford Protein assay (Bio-Rad) using bovine serum albumin as a standard. All *E. coli* expression vectors and strains were from Stratagene. The yeast expression vector pDB20 was provided by Dr. L. Guarente (Massachusetts Institute of Technology). When noted, argon supplies were scrubbed by passing the gas stream through a solution of pyrogallol (Sigma) containing a few pellets of KOH.

Mutagenesis and Purification of Mutants Expressed in S. cerevisiae. Mutagenesis of the amine oxidase from *H. polymorpha* was performed as described by Cai and Klinman (*2*) or by using the Chameleon Kit from Stratagene. The latter kit is based on a modification of the unique elimination mutagenesis procedure detailed by Deng and Nickoloff (*18*). Selection of mutant vs WT DNA was accomplished by mutating the unique *Aat*II site in pDB20 using the oligonucleotide 5′-GGTTTCTTAGACGACAGGTGGCACTTTTC-3′ as a primer. The sequences for the synthetic mutagenic oligonucleotides were 5′-CGAGATGATTGTTCCT**GC**CG-GCTCGCCAGAG-3′, 5′-GATTGTTCCTT**G**CGGCTCGC-CAGAG-3′, and 5′- GATTGTTCCT**TT**GGCTCGCCA-GAG-3′ for mutants Y305A, Y305C, and Y305F, respectively. The mutated nucleotides are shown in boldface and the mutated codons underlined. Expression in *S. cerevisiae* and purification procedures were as described by Cai and Klinman (*3*) with two modifications: in some cases, the ammonium sulfate step was omitted, and for fractions that were less than 95% pure, the Mono-Q step was included.

Domain Analysis. Limited proteolysis of HPAO proteins was accomplished using a slightly modified procedure of Plastino and Klinman (*19*). Approximately 10 μg of HPAO protein was incubated with 4% (w/w) V-8 protease in 100 mM potassium phosphate buffer, pH 7.8, with 1 M urea at 37 °C. At the designated times, aliquots were removed, quenched with 23 mM phenylmethylsulfonyl fluoride, and quickly frozen in liquid nitrogen until analyzed by SDS−PAGE.

Cloning and Purification of Cu-Free Y305A Precursor Protein from E. coli. The pET11a-derived pKW3 expression vector (*6*) containing WT HPAO was partially digested with *Eag*I under conditions that maximized the yield of the desired 5.7 kb linearized vector. Approximately 3 μg of pKW3 was

[3] *Hansenula polymorpha* has been reclassified as *Pichia angusta* (*1*).

[4] The term productive conformation refers to an active-site geometry which is ready for catalysis, as indicated by the positioning of the C-5 carbonyl near the active-site base. The term nonproductive conformation refers to those active-site geometries either which are not ready for catalysis (i.e., the C-5 carbonyl is pointed away from the active-site base) or which result in the build-up of intermediates or dead end complexes. An inactive conformation is a geometry of the active site which is unable to react with substrate.

digested with 40 units of *Eag*I for 35 min at 37 °C. In addition to the 5.7 kb band of interest, a 6 kb band representing the WT HPAO gene plus a small portion of the vector copurified from the agarose gel. The mixture of fragments was ligated with the gene for Y305A, which had been removed from the yeast expression vector pDB20 via an *Eag*I digest. Plasmids resulting from the transformation of XL1-Blue were screened using restriction digests. The resultant expression plasmid contained the *H. polymorpha* sequence commencing at codon 13 (*20*) with the Y305A mutation and was used to transform BL21(DE3) for protein expression. *E. coli* cell culture and protein purification procedures were performed using established methodology (*6*).

Protein Characterization Methods. The amount of TPQ was determined by end-point titration with a 10-fold molar excess of [U-^{14}C]phenylhydrazine (specific activity 2.5 mCi/mmol) (*3*). Labeling was monitored using a Hewlett-Packard 8452A diode-array spectrophotometer. After the absorbance at 440 nm reached a maximum value, unreacted phenylhydrazine and protein were separated on a DG-10 gel filtration column (Bio-Rad). The radioactivity in the protein fraction was counted, and a new spectrum was collected. The extinction coefficients for each of the mutants were calculated based on the amount of radiolabeled phenylhydrazone formed, the final absorbance value at 440 nm in the desalted sample, and the protein concentration based on a subunit M_r = 75 700. Metal analysis for copper and zinc was performed by standard addition atomic absorption spectroscopy (*2*) and/or inductively coupled plasma (ICP) emission spectroscopy (*6*). Redox-cycling staining was performed as described previously (*21*).

Steady-State Kinetic Measurements. All assays were initiated with enzyme and carried out at 25 °C for WT HPAO using methylamine or at 37 °C for WT HPAO with benzylamine and Y305 mutants unless otherwise indicated. Initial rates were fitted to the Michaelis−Menten equation using nonlinear regression. Maximum velocity values were converted to k_{cat} values by correcting for the amount of TPQ present in each protein preparation. (1) Reductive half-reaction: The rate of benzylamine amine oxidation was followed as a function of benzaldehyde formation at 250 nm as described previously (*17*). The K_m of oxygen in Y305A is severely perturbed with benzylamine as the substrate (~250 μM at pH 7); therefore, the k_{cat} for benzylamine oxidation was approximated by using the maximum velocity at saturating oxygen projected by nonlinear regression of activity data as a function of oxygen concentration. Aliphatic amine substrates were analyzed by measuring the rate of oxygen consumption using a Clark oxygen electrode (Yellow Spring Instrument). All results in Tables 1 and 2 were obtained from air-saturated 100 mM potassium phosphate buffer, pH 7, ionic strength = 175 mM, with the exception of the Y305F assays. Since Y305F activity at pH 7 was barely detectable above noise, catalysis by this mutant was measured at pH 8 using 65 mM potassium phosphate, ionic strength = 175 mM, and the kinetic parameters were interpolated to pH 7 using the pH curves obtained with Y305A, assuming the same pH dependence for Y305F. In Table 2, k_{cat}/K_m for oxygen was determined with 5 mM ethylamine or 10 mM benzylamine. (2) Oxidative half-reaction: The rate of oxygen consumption was studied as a function of oxygen concentration using the Clark electrode. Solutions (1 mL) were equilibrated to a known concentration of oxygen by passing mixtures of N_2 and O_2 over the solution while stirring. Assays were performed in 100 mM potassium phosphate, pH 7.2, ionic strength = 198 mM, using saturating concentrations of amine and initiated with enzyme via a gastight syringe. (3) pH profiles: Measurements of the pH dependencies of kinetic parameters with methylamine and benzylamine were carried out for WT enzyme at 25 and 37 °C, respectively, and employed the following buffers: 100 mM potassium phosphate (pH 5.95−8.01), 25 mM potassium pyrophosphate (pH 7.66−9.14), and 100 mM potassium carbonate (pH 9.02−9.96). KCl was used to maintain the ionic strength at 300 mM when methylamine was used and at 350 mM when benzylamine was used. Y305A activity was measured at 37 °C with methylamine and ethylamine. At pH values less than 7.2, the Y305A reactions were carried out in oxygen-saturated buffer to maintain a ≥10-fold excess of oxygen. Log k_{cat} and log(k_{cat}/K_m) were plotted vs pH and fitted to one of the following equations (*22*):

$$\log(k_{cat}) = \log(k_{cat})_{max} - \log(1 + 10^{pK_{a1}-pH} + 10^{pH-pK_{a2}}) \quad (3)$$

$$\log(k_{cat}/K_m) = \log(k_{cat}/K_m)_{max} - \log(1 + 10^{pK_{a1}-pH} + 10^{pH-pK_{a2}}) \quad (4)$$

Kinetic isotope effects measured with WT HPAO were extracted from the pH curves described above. Kinetic isotope effects with Y305C were measured in air-saturated, 100 mM potassium phosphate adjusted with KCl to maintain the ionic strength at 350 or 300 mM for the benzylamine and methylamine studies, respectively.

Pseudo-First-Order Spectral Studies. Methylamine and ethylamine oxidation by Y305A was monitored spectrophotometrically under pseudo-first-order conditions. Assays were performed at pH values of 6.46 and 7.57 with 100 mM potassium phosphate and at pH 9.45 with 100 mM potassium carbonate. Constant ionic strength was maintained at 300 mM with KCl. After obtaining a stable spectrum of resting enzyme (typically 107 μg of Y305A containing 71% TPQ in 120 μL), enough methylamine or ethylamine was added to maintain pseudo-first-order conditions for at least 2 min, and scans were taken at 15 s intervals. The first spectrum was typically taken within 15 s of adding substrate. Methylamine and ethylamine oxidation was followed at 20 and 10 °C, respectively. Spectral studies at pH 6.46 also employed a cuvette fitted with a septum and an oxygen-filled balloon to maintain a saturating concentration of oxygen.

TPQ Biogenesis. Copper-free Y305A precursor protein was reconstituted in 50 mM HEPES, pH 7.2, with an equimolar amount of either $CuCl_2$ or $CuSO_4$ using specific conditions as indicated in the text. Absorbance changes that occurred during TPQ formation were monitored using a Hewlett-Packard 8452A diode-array spectrophotometer equipped with a thermostated cell holder. The absorbance data at 500 nm (excluding an apparent 100 min lag phase) were fitted to a single exponential (eq 5) to obtain k_{obs} for the formation of TPQ. All presented spectra and rates were

$$Abs_{500} = C(1 - e^{-kt}) + b \quad (5)$$

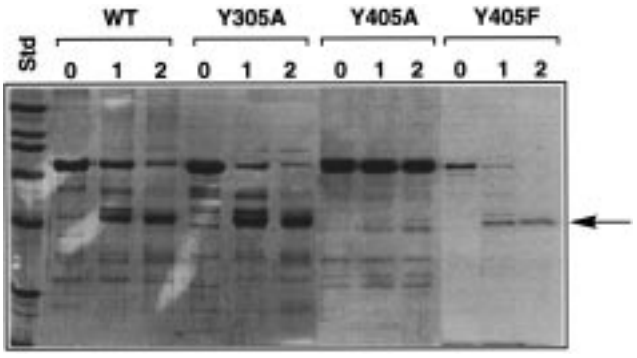

FIGURE 1: Domain analysis of WT HPAO and HPAO mutants by limited proteolysis. Molecular mass markers of 200, 116, 97.4, 66, 45, 31, and 21.5 kDa are shown in the first lane. Samples of the different proteins were digested for 0, 1, and 2 h as described under Experimental Procedures. The arrow marks the molecular mass of the 48 kDa digest product.

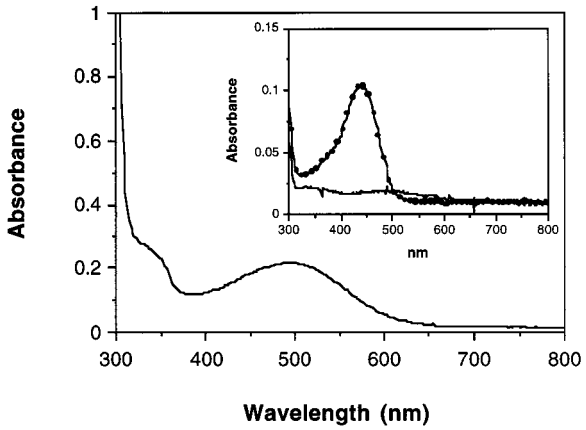

FIGURE 2: UV−Vis spectra of 12 mg/mL yeast-expressed Y305A containing 61% TPQ. The inset is the corresponding phenylhydrazone derivative of a 0.44 mg/mL sample (solid line, resting enzyme; line with data points, phenylhydrazone derivative).

normalized at either 720 or 800 nm. Anaerobic addition of Cu^{2+} was performed using a hand-crafted cuvette having a bulbous top and ground glass joint. An initial spectrum of apo-enzyme was taken, the headspace in the cuvette was purged quickly with scrubbed argon, and a septum was attached. The cuvette was placed on ice and tilted so that the protein solution (up to 400 μL) flowed into the bulbous part of the cuvette. Scrubbed argon was then blown over the surface of the protein solution with occasional swirling for 25 min. Prior to adding anaerobic cupric ion solutions via a gastight syringe, the cuvette and its contents were allowed to equilibrate to the desired temperature in the cell holder for up to 15 min. The measurement of TPQ content was as described above. Specific activity was measured at 37 °C in 100 mM potassium phosphate, pH 7, using 9 mM benzylamine. The copper and zinc content of reconstituted Y305A was performed on dialyzed protein using the methods described above.

RESULTS

Domain Analysis

Limited proteolysis of HPAO was first utilized by Plastino and Klinman (*19*) to identify a C-terminal, 48 kDa domain consisting of the copper binding site and the TPQ consensus sequence. Based on this earlier study, we developed a screening procedure using domain analysis to identify HPAO proteins which had folded improperly. Partial digestion of WT HPAO results in a characteristic 3-band pattern consisting of undigested protein at 72 kDa and a doublet around 48 kDa. (Figure 1). In a series of active-site mutants, made for a different set of experiments, mutations at Y405 resulted in a different, size-dependent pattern of proteolysis. Although Y405F is susceptible to proteolysis and demonstrates the 3-band digest pattern, Y405A is not susceptible to cleavage under the same conditions (Figure 1). Y405G is also not susceptible to proteolytic cleavage, while increasing the size of the side chain to Val or Leu leads to normal proteolysis (data not shown). These results indicate a difference in the conformation of the site of proteolytic cleavage in Y405A and Y405G and, thus, suggest an altered folding pattern for these mutants. To decrease the possibility that mutations at Y305 alter TPQ biogenesis and/or amine oxidase activity by affecting the global structure of HPAO, this type of domain analysis was performed on Y305A, Y305C, Y305F, and apo-Y305A. As typified by Y305A (Figure 1), all Y305 mutants demonstrated normal digestion patterns.

Characterization of Y305 Mutants Expressed in Yeast

General Properties. Although all three Y305 mutants purified like WT HPAO, it was noted early in the purification procedure that some crude lysates of Y305A did not produce a redox stain (data not shown). This did not appear to be due to an inhibition of the staining procedure, as crude extracts that were spiked with WT HPAO produced a redox stain as normal. Semipurified and purified samples of all three mutants did show a positive redox stain, indicating the presence of TPQ in the later stages of purification. This was the first piece of evidence suggesting that biogenesis might be altered in Y305A. The purified proteins reacted positively with antibodies raised against WT HPAO, demonstrated normal proteolysis patterns (as discussed above), and contained one Cu atom per subunit as shown by metal analysis.

The UV−Vis spectra of all mutants were similar to that of WT protein with a λ_{max} at 495 nm corresponding to TPQ and a shoulder in the 340 nm range (Y305A is shown in Figure 2). The amount of TPQ was quantified by derivatizing protein with phenylhydrazine to form the highly chromophoric phenylhydrazone (λ_{max} = 450 nm in WT). Using WT protein, this reaction proceeds quickly, reaching an end point in ~25 min at 25 °C with the resulting phenylhydrazone having an extinction coefficient of 40 500 M^{-1} cm^{-1} (*3*). Phenylhydrazine derivatization of the Y305 mutants was much slower; derivatizations of both Y305A and Y305C required 30−45 min at 37 °C to reach completion, resulted in a λ_{max} which was slightly blue-shifted to 440 nm, and indicated the presence of substoichiometric amounts of TPQ. Derivatization of the mutants with [^{14}C]phenylhydrazine, to quantify the amount of phenylhydrazone, yielded a reduced extinction coefficient of 25 000 M^{-1} cm^{-1} for Y305A and Y305C. In the case of preparations of Y305C, this led to a ratio of TPQ to protein subunit of 0.59:1, or 59%, while individual preparations of Y305A varied in TPQ content from 48 to 72% (see Figure 2, inset). Based on the amount of TPQ present, the extinction coefficient at 495 nm for underivatized Y305A and Y305C was estimated at 1700 M^{-1} cm^{-1}, compared to approximately 2400 M^{-1} cm^{-1} for WT

Table 1: Relative Rates for Ethylamine Oxidation by WT HPAO and Y305 Mutants at pH 7[a]

enzyme	k_{cat} (s^{-1})[b]	k_{cat}/K_m (M^{-1} s^{-1})[b]
WT	20	5.2×10^4
Y305A	7.5 (0.4)	1.4×10^4 (0.3)
Y305C	4.7 (0.2)	0.74×10^4 (0.1)
Y305F[c]	0.16 (0.008)	0.01×10^4 (0.002)

[a] 100 mM potassium phosphate, ionic strength of 175 mM; 37 °C. [b] Rates relative to WT are in parentheses. [c] Rates were measured in 65 mM potassium phosphate at pH 8, ionic strength of 175 mM, and extrapolated to pH 7 using the pH curves obtained with Y305A.

HPAO (*23*). The reduced extinction coefficient is similar to that seen with mutations of HPAO made at the proposed active-site base (Asp319) (*23*). Similar studies with Y305F yielded more complicated results. First, the rate of phenylhydrazine derivatization was noticeably slower than with the other two mutants; even after 1.5 h, the absorbance at 440 nm was still increasing. Second, due to the decreased rate of reaction, an end point was not reached before side reactions started to occur which obscured the spectra. Although the exact TPQ content could not be determined, it was estimated that the ratio of TPQ to protein subunit was at least 0.3:1. It is noteworthy that yeast-expressed WT HPAO has also been found to contain substoichiometric amounts of cofactor capable of reacting with phenylhydrazine (ranging from 70 to 98%). The origin of this effect and the chemical nature of the active site in the fraction of protein which does not react with phenylhydrazine remain unknown. It is, thus, not possible to ascribe the substoichiometric TPQ values determined for the Y305 mutants to the altered active site. Some differences in the electronic structure of TPQ in the mutants are, however, indicated by changes in the TPQ extinction coefficient. Preliminary resonance Raman data on Y305A and Y305F also indicate differences in the spectra of TPQ in the mutants compared to TPQ in WT HPAO (*24*).

Amine Oxidase Activity. Mutations at Y305 alter amine oxidase activity in two ways. First there is a substitution-dependent decrease in activity, illustrated in Table 1. Y305A and Y305C behave similarly with aliphatic amine substrates (ethylamine results are shown in Table 1), demonstrating modest 3−7-fold decreases in k_{cat} and k_{cat}/K_m for amine at pH 7. Analysis of the oxidative half-reaction yielded similar trends. The most significant effect was seen with the Phe substitution; ethylamine oxidation by Y305F was severely impaired as demonstrated by the >100-fold decrease in k_{cat} and >500-fold decrease in k_{cat}/K_m for the reductive half-reaction. It should be noted that these kinetic parameters are based on a lower limit estimation of the TPQ content of Y305F. If the TPQ content was underestimated, the values for k_{cat} and k_{cat}/K_m would be even smaller. The K_m for oxygen for Y305F with ethylamine as substrate was less than 5 μM, indicating that the large decrease in k_{cat} and k_{cat}/K_m for substrate was not due to lack of saturation with oxygen.

Table 2 illustrates the second effect of mutating Y305. In catalysis by WT HPAO, aliphatic amines are preferred over benzylamine as indicated by the >200-fold larger k_{cat}/K_m for amine (*2*). With Y305A the difference in efficiency is magnified to >700-fold due to the substantial decrease in the ability of Y305A to catalyze benzylamine oxidation. This was also observed with the Y305C mutant (data not shown). Further analysis revealed that when benzylamine is used as the substrate with Y305A the K_m for oxygen increases more than 100-fold from 2 μM to ≥250 μM and k_{cat}/K_m decreases more than 1000-fold. Thus, the net result of the mutation was to increase the substrate specificity for aliphatic amines. Based on the evidence for ping-pong kinetics among the CAOs, it was expected that the behavior of Y305A would approximate a ping-pong mechanism. However, we find a very large, benzylamine-specific effect on the oxidative half-reaction. One proposal that arose during these studies was that product benzaldehyde may bind particularly well into a pocket created by deletion of the phenyl ring in Y305A. Although attempts to inhibit activity of Y305A with benzaldehyde failed (data not shown), it is possible that aldehyde can only reach its targeted site if generated *in situ*. As an alternative explanation, the Y305A enzyme may be especially sensitive to benzylamine inhibition at the concentration of benzylamine used (10 mM) in the determination of k_{cat}/K_m for oxygen.

Table 2: Substrate Specificity for WT HPAO and Y305A at pH 7[a]

substrate/parameter	WT	Y305A[b]
ethylamine		
k_{cat} (s^{-1})	20	7.5 (0.4)
$k_{cat}/K_{m,amine}$ (M^{-1} s^{-1})	5.2×10^4	1.4×10^4 (0.3)
$k_{cat}/K_{m,oxygen}$ (M^{-1} s^{-1})[c]	6.6×10^5	1.3×10^5 (0.2)
benzylamine		
k_{cat} (s^{-1})	0.26	~0.032 (0.12)[d]
$k_{cat}/K_{m,amine}$ (M^{-1} s^{-1})	0.022×10^4	0.0006×10^4 (0.03)
$k_{cat}/K_{m,oxygen}$ (M^{-1} s^{-1})[c]	1.3×10^5	$\leq 0.0013 \times 10^5$ (0.001)

[a] 100 mM potassium phosphate, ionic strength of 175 mM; 37 °C. [b] Rates relative to WT are in parentheses. [c] Rates were measured at pH 7.2, ionic strength of 350 mM, [ethylamine] = 5 mM, [benzylamine] = 10 mM. [d] k_{cat} was approximated as described under Experimental Procedures.

pH Dependence of the Reductive Half-Reaction and Kinetic Isotope Effects. A few kinetic parameters for yeast-expressed WT HPAO were reported by Cai and Klinman (*3*); however, this is the first detailed kinetic study of this enzyme. Using methylamine as a substrate, WT HPAO shows ping-pong kinetics as indicated by parallel lines in a double-reciprocal plot (data not shown).

The pH profiles of substrate oxidation by WT HPAO are shown in Figures 3 and 4. The plots of $\log(k_{cat}/K_m)$ for amine vs pH are bell-shaped. Using methylamine as the substrate, the plots show pK_a's of 8.1 ± 0.1 and 9.9 ± 0.2 (Figure 3A). Benzylamine oxidation shows a similar shape within the pH range that can be studied. Low reactivity of HPAO below pH 7.3 prevents data collection below this pH. pK_a's cannot be determined from eq 2 due to inhibitory effects of the carbonate buffer not seen with methylamine. The isotope effect on k_{cat}/K_m for both substrates is about 4.5 and is pH-independent for methylamine and possibly for benzylamine (Figure 3B,D).

We attribute the pK_a's in k_{cat}/K_m for amine to an active-site base on the enzyme (K_a) and to the substrate (K_s), respectively (Scheme 4). A pK_a of about 8 was seen previously with BSAO (*25*) and was attributed to an active-site base which must be deprotonated for the reaction to occur. The pK_a's of methylamine and benzylamine are 10.6 and 9.3, respectively (*26*). The higher pK_a in the k_{cat}/K_m profiles is assigned to the substrate which interacts with the enzyme in its protonated form. The deprotonated active-site base is expected to act as a general base toward protonated substrate in the formation of the substrate Schiff base complex. It is now clear from the crystal structures of CAOs

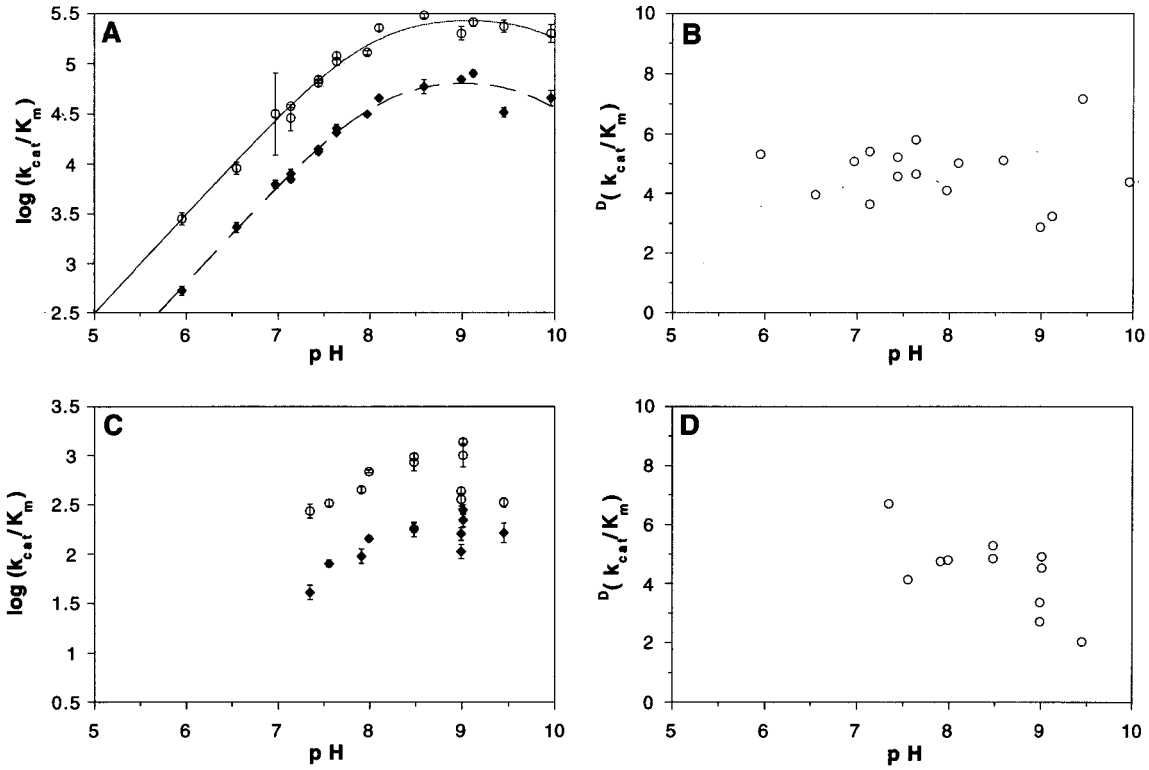

FIGURE 3: pH profiles and isotope effects on k_{cat}/K_m for methylamine (A and B) and benzylamine oxidation (C and D) by WT HPAO. Initial rates of both protio (open circles) and deutero (closed diamonds) substrate oxidation were measured at 25 °C using an oxygen electrode for methylamine or at 37 °C spectrophotometrically for benzylamine as described under Experimental Procedures. Standard errors are shown with error bars when they are bigger than the symbols. The units of k_{cat}/K_m are given as M^{-1} s^{-1}. The data were fit to eq 2 (Experimental Procedures). The values for the fits of the methylamine data are as follows: H-MeAm, pK_{a1} = 8.0 ± 0.1 and pK_{a2} = 10.1 ± 0.3; D-MeAm, pK_{a1} = 8.1 ± 0.1 and pK_{a2} = 9.9 ± 0.2.

that the active-site base is an aspartate [Asp 319 in HPAO (*15*)] and, from the present study, that the pK_a for this group is very similar in HPAO and BSAO (*25*). A characteristic of HPAO that is different from BSAO is the isotope effect on k_{cat}/K_m; $^{d}(k_{cat}/K_m)$ was reported to be 12 for BSAO (*25*) while for HPAO it is reduced to 4.5 (Figure 3B,D). This suggests that the reductive half-reaction is significantly more limited by C−H bond cleavage in the BSAO reaction. It is also possible (although we consider it unlikely) that the intrinsic isotope effect for HPAO is less than that of BSAO.

The plot of log k_{cat} vs pH is also bell-shaped with methylamine (Figure 4A), showing pK_a's of 7.9 ± 0.1 and 8.8 ± 0.1. The plot with benzylamine indicates a much smaller pH dependence, precluding pK_a determination (Figure 4C). In contrast with BSAO, the isotope effects on k_{cat} for HPAO with both substrates are smaller, indicating that k_{cat} for HPAO is less rate-limited by C−H bond cleavage than is BSAO. Interestingly, the isotope effects determined with methylamine and benzylamine are different; methylamine shows an average isotope effect of 1.2 that may be slightly pH-dependent (Figure 4B), while the isotope effect with benzylamine decreases slightly from 4.5 to 3 with increasing pH (Figure 4D). This indicates that C−H bond cleavage is significantly more rate-limiting of k_{cat} for benzylamine than methylamine with WT HPAO.

The pH profile of methylamine oxidation by Y305A is very different from that of WT HPAO. Although the plot of log k_{cat} vs pH is bell-shaped, k_{cat} begins to decrease at pH values >7, giving rise to pK_a values of 6.5 ± 0.15 and 6.9 ± 0.09 (Figure 5A), compared to 7.9 and 8.8 determined for WT. Curvature in the initial velocity traces of methylamine oxidation by Y305A started at pH >7 and increased with pH (data not shown). The effect on k_{cat} is specific for methylamine, since the pH profile for ethylamine oxidation (Figure 5A) is similar to that of methylamine oxidation by WT HPAO. Interestingly, although k_{cat} decreased above pH 7 in methylamine oxidation, k_{cat}/K_m values continued to increase (Figure 5B), mimicking the profile obtained for ethylamine. Kinetic isotope effects on k_{cat} of 1.2 and k_{cat}/K_m of 4.3 determined with deuterated methylamine at pH 7.4 are similar to those obtained for WT HPAO. Above pH 8 the K_m for methylamine became too small to measure (K_m = 3 μM at pH 8.0); therefore, a good fit of the log(k_{cat}/K_m) vs pH data could not be made. On the other hand, ethylamine oxidation could be followed up to pH 10 (Figure 5B), yielding pK_a values of 8.2 ± 0.09 and 9.8 ± 0.20. A pH profile for benzylamine oxidation by Y305A was not attempted due to the low turnover for this substrate and the inability to saturate with oxygen over the pH range. Overall, the pH profiles for WT HPAO and Y305A demonstrate very similar pH sensitivities with the exception of the oxidation of methylamine by Y305A.

Methylamine-Derived Schiff Base Formation in Y305A at High pH. The source for the pH-dependent decrease in k_{cat} for methylamine oxidation with Y305A was studied by comparing spectra obtained during turnover at a pH where k_{cat} was still increasing and at a pH where k_{cat} was decreasing. At pH 6.46, addition of methylamine to Y305A resulted in the immediate bleaching of oxidized cofactor absorbance at 500 nm (Figure 6A). The resulting spectrum is very similar to those obtained by Mure and Klinman (*27*) for 6-amino-4-ethylresorcinol, a model compound of the proposed ami-

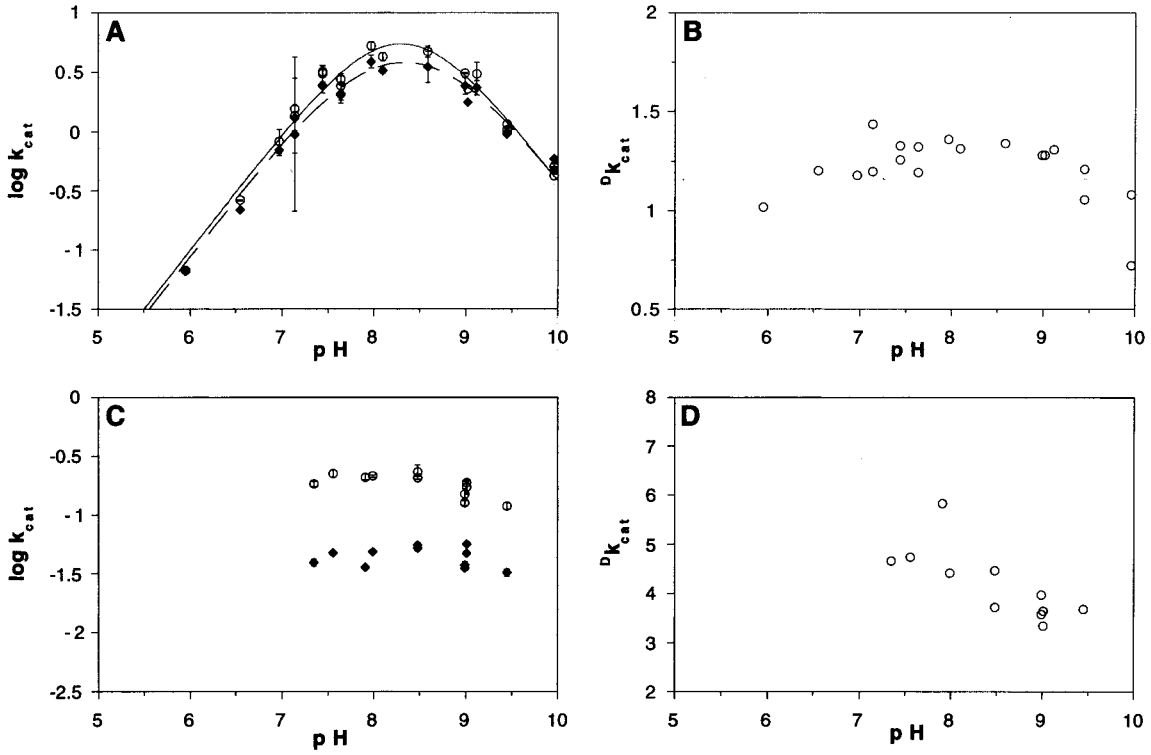

FIGURE 4: pH profiles and isotope effects on k_{cat} for methylamine (A and B) and benzylamine oxidation (C and D) by WT HPAO. Initial rates of both protio (open circles) and deutero (closed diamonds) substrate oxidation were measured at 25 °C using an oxygen electrode for methylamine or at 37 °C spectrophotometrically for benzylamine as described under Experimental Procedures. Standard errors are shown with error bars when they are bigger than the symbols. The units of k_{cat} are given as s^{-1}. The data were fit to eq 1 (Experimental Procedures). The values for the fits of the methylamine data are as follows: H-MeAm; pK_{a1} = 8.1 ± 0.2 and pK_{a2} = 8.5 ± 0.2; D-MeAm; pK_{a1} = 7.9 ± 0.1 and pK_{a2} = 8.8 ± 0.1.

Scheme 4: Kinetic Mechanism for Amine Oxidation by HPAO, Including Ionizations Required To Explain Results in both k_{cat}/K_m and k_{cat}

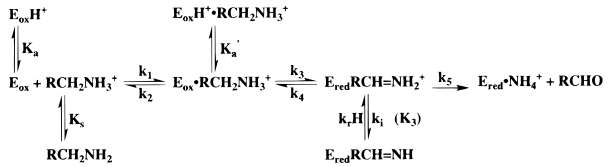

nophenol reaction intermediate. At pH 7.57, where k_{cat} is decreasing, addition of methylamine to Y305A resulted in the incomplete bleaching of the cofactor absorbance and the appearance of a new shoulder at 388 nm (Figure 6B). This spectrum is almost identical to that obtained by Cai and coworkers (*28*) for the stable, methylamine-derived, product Schiff base that is formed with the active-site mutant E406N. In the case of E406N, formation of the product Schiff base occurred slowly and led to an accumulation of inhibited enzyme. However, the peak at 388 nm for Y305A was only observed under pseudo-first-order conditions and quickly disappeared as >10% of the substrate was consumed. The buildup of the spectral intermediate was also seen with Y305F at pH 7.57 (data not shown), suggesting a common phenomenon in methylamine oxidation for mutations made at position 305. Importantly, this intermediate was not observed when ethylamine was the amine substrate (data not shown). We note that while the E406N intermediate was unequivocally identified as the deprotonated product Schiff base by resonance Raman spectroscopy (*28*), the Y305 intermediates have only been characterized by UV−Vis properties, due to their much shorter lifetimes. However, observation of a 388 nm peak with methylamine, but not with larger substrates such as ethylamine, is similar for Y305A and E406N; as postulated by Cai et al. (*28*), the greater bulk of the product Schiff base with ethylamine prevents reorientation of the cofactor into a nonproductive binding mode.

A significant difference between Y305A and E406N is that E406N shows initial velocity traces which are very similar to WT over the pH range studied, while above pH 7, values for k_{cat} with Y305A are reduced significantly from WT. A possible explanation for this effect with Y305A is shown in Scheme 4, where K_a and K_a' refer to the ionization of the active-site base in the free enzyme and in the substrate Schiff base complex, respectively, and K_s is the ionization of free substrate [cf. Farnum et al. (*25*) for a similar description of ionization processes with BSAO]. With the Y305A mutant of HPAO, we include a rapid, pH-dependent isomerization of the product Schiff base (k_i) into a nonproductive conformation as the cause of the falloff in rate above pH 7 and the short lifetime of the 388 nm species. This ionization may reflect deprotonation of the product Schiff base as illustrated or possibly another protein-bound functional group. In the case of E406N, the pH dependence for the much slower isomerization was ascribed to an active-site His which had undergone a large decrease in its pK_a relative to WT enzyme due to loss of the counterion (Glu406) in the mutant (*28*).

Characterization of TPQ Biogenesis in Y305A. Previous studies have shown that the expression of the apo-precursor form of WT HPAO in *S. cerevisiae* is not feasible due to zinc incorporation, whereas expression in *E. coli* allows for

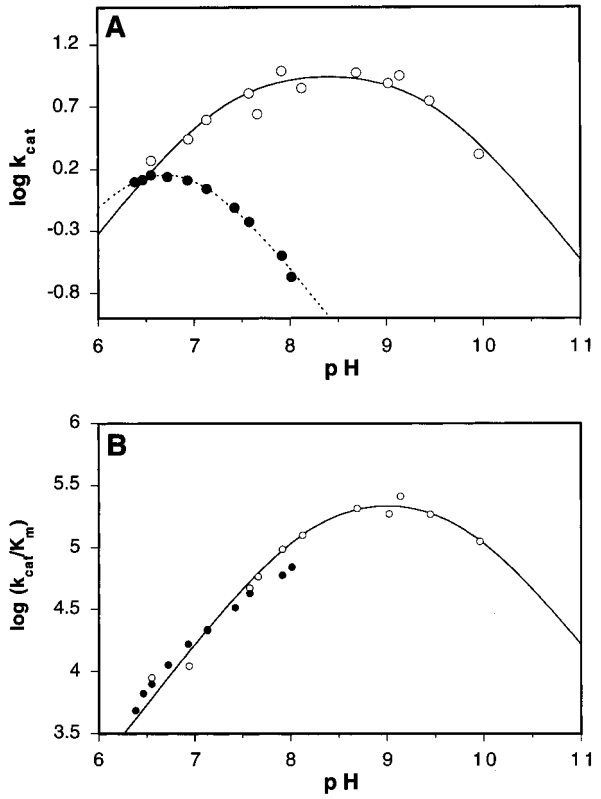

FIGURE 5: pH profiles for the reactions of methylamine (solid circles) and ethylamine (open circles) with Y305A. Initial rates were measured at 37 °C using an oxygen electrode as described under Experimental Procedures. Standard errors are shown with error bars when they are bigger than the symbols. The parameters of k_{cat} and k_{cat}/K_m are given as s^{-1} and M^{-1} s^{-1}, respectively. Data in (A) were fit to eq 1, and ethylamine data in (B) were fit to eq 2 (Experimental Procedures). The values for the fits are the following: k_{cat}, methylamine, pK_{a1} = 6.5 ± 0.15 and pK_{a2} = 6.9 ± 0.08; k_{cat}, ethylamine, pK_{a1} = 7.3 ± 0.13 and pK_{a2} = 9.5 ± 0.16; and k_{cat}/K_m, ethylamine, pK_{a1} = 8.2 ± 0.09 and pK_{a2} = 9.8 ± 0.20.

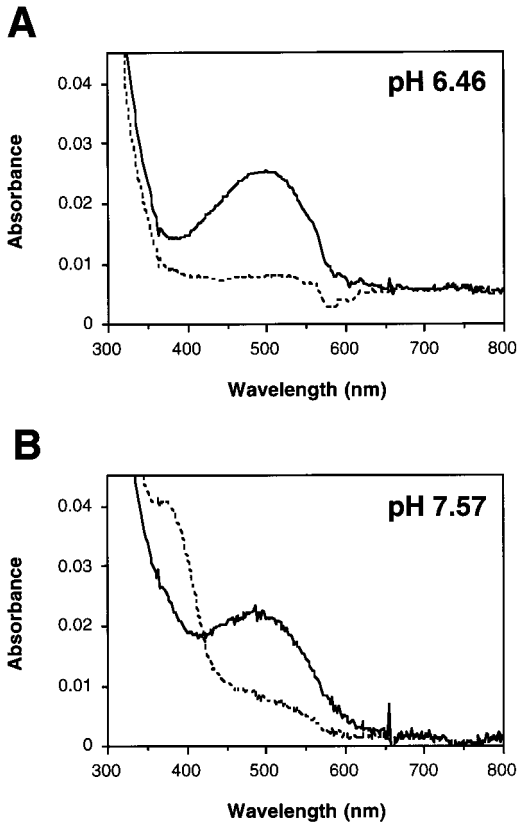

FIGURE 6: Methylamine-derived product Schiff base formation at high pH under pseudo-first-order conditions. Y305A (0.89 mg/mL containing 71% TPQ) was equilibrated to 20 °C at the specified pH, and a spectrum of the resting enzyme was taken (solid line). Methylamine was added to the cuvette at a final concentration of 2.9 mM in (A) or 1.9 mM in (B), and a series of spectra were taken. Spectra taken under pseudo-first-order conditions are represented by the dashed lines.

the easy isolation of Cu- and TPQ-free WT HPAO (*6*). Likewise, it was found that the apo-precursor form of Y305A could only be isolated from an *E. coli* expression system. The purified mutant produced a normal limited proteolysis pattern, stained positively in Western analysis, and did not produce a redox stain (data not shown). The enzyme was also void of any chromophore, did not exhibit any benzylamine oxidase activity, and contained less than 1.5% copper and no observable zinc. Taken together the data suggested the purification of a properly folded apo-precursor HPAO.

Following conditions used for reconstituting WT HPAO (*6*), the apo-precursor form of Y305A was incubated at 20 °C in the presence of Cu^{2+}. Spectra recorded over a 15 h time period demonstrated an increase in absorbance at 500 nm (Figure 7A) consistent with the formation of TPQ, but at a rate much slower than that of WT HPAO. There was a short lag, followed by an increase in absorbance at 500 nm (Figure 7B) which could be fit to a single exponential to yield a $k_{obs} = 1 \times 10^{-4}$ min^{-1} compared to approximately 0.085 min^{-1} for WT HPAO (*29*). An experiment using a higher concentration of oxygen demonstrated relatively little effect on the rate of biogenesis in Y305A, suggesting that a much altered K_m for oxygen was not the reason for the reduced rate of biogenesis (data not shown). Even though the rate of TPQ biogenesis was impaired, the final content of TPQ in Y305A approached that of reconstituted WT HPAO. Periodic analysis of samples kept at 4 °C showed that biogenesis had stopped after ~3−4 weeks with 50−60% TPQ. Although a full kinetic study was not done, reconstituted Y305A having 61% TPQ was shown to be active with a specific activity for benzylamine oxidation of 3.9×10^{-3} unit/mg, which is similar to the specific activities of $(3-4) \times 10^{-3}$ unit/mg measured for yeast-expressed Y305A with 62% TPQ. Copper analysis of dialyzed, reconstituted Y305A demonstrated the presence of stoichiometric Cu and less than 5% Zn. Thus, the inability to achieve 100% TPQ was not due to incomplete copper incorporation.

Examination of the absorbance changes that occur over time during the reconstitution (Figure 7B) also shows changes in absorbance at 380 nm. The trace at 380 nm is consistent with the formation of at least two species. The first is formed rapidly and reaches a maximum within about 1000 s (arrow). The second increases slowly throughout the rest of the reconstitution. The initial absorbance at 380 nm has also been documented during the reconstitution of apo-WT HPAO, where the absorbance change has been shown to represent an oxygen-independent, transient event, with the absorbance at 380 nm returning to baseline (*29*). Further studies demonstrated that the initial increase in absorbance at 380 nm was oxygen-independent in Y305A. Once the anaerobic system was exposed to oxygen, the formation of TPQ proceeded at the expected rate without any lag in the absorbance at 500 nm (data not shown).

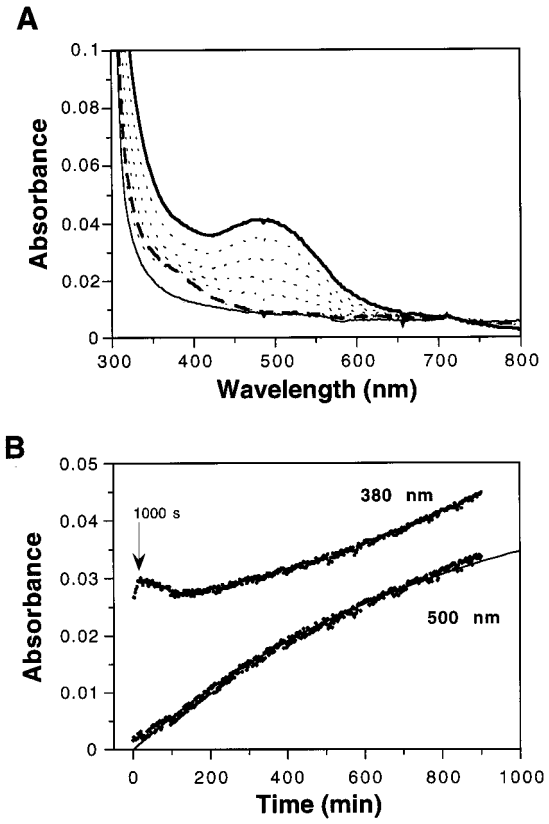

FIGURE 7: TPQ formation in *E. coli*-expressed apo-Y305A. (A) 40 μM apo-Y305A in 50 mM HEPES, pH 7.2, was equilibrated to 20 °C, and a spectrum was collected (solid thin line). 40 μM $CuCl_2$ was added to the sample, and spectra were taken immediately after the addition (bold dashed line) and then several times over 15 h (dotted lines, intermediate spectra; bold solid line, final spectrum). (B) Changes in absorbance at 380 nm (data have been offset by +0.01 absorbance unit for clarity) and 500 nm (solid line) over time. All data were normalized at 720 nm. After excluding the first 100 min of the reaction, the data obtained at 500 nm in (B) were fit to a single exponential to give a value for $k_{obs} = 1 \times 10^{-4}$ min^{-1}.

Finally, as was noted under Experimental Procedures, the apo-precursor form of Y305A is not a stable protein. Reconstitutions performed at 30 °C result in a substantial amount of baseline shift in the 350−450 nm range of the spectra (data not shown). Although the extent of biogenesis, as indicated by TPQ content and/or benzylamine activity did not appear significantly different from that of protein reconstituted at 20 °C, rate data were difficult to analyze due to overlapping absorbances. Prolonged storage (>2 months) of apo-precursor Y305A at either 4 °C or −20 °C had the same effect as increasing the reconstitution temperature; i.e., spectral changes during the reconstitution were not as well-defined. Also, the rate of TPQ biogenesis appeared to decay with prolonged storage.

DISCUSSION

In this study, we have examined the role of the strictly conserved, active-site tyrosine (Tyr305 in HPAO) which resides within close hydrogen-bonding distance of the C-4 oxygen of the TPQ cofactor. The first crystal structure of a CAO [phenethylamine oxidase from *E. coli* (*13*)] indicated that Tyr305 was in close proximity to the TPQ ring. A recent structure of HPAO, the first CAO structure for which the cofactor resides in a catalytically productive conformation, indicated that the C-4 oxygen was close enough to Tyr305

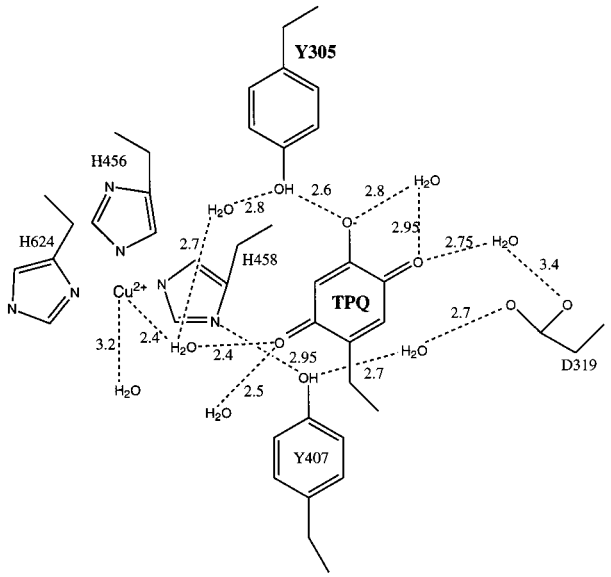

FIGURE 8: Schematic of key residues in the active site of HPAO *(12)*.

to force the C-4 hydroxyl out of planarity with the rest of the benzene ring (*15*). This tyrosine can also be seen to provide a key hydrogen bond in a network of H-bonds which links the two (separate) regions of the active site catalyzing substrate oxidation and dioxygen reduction, respectively (Figure 8).

Nonproductive Conformations of TPQ. One feature that has begun to dominate our investigations of active-site mutants of HPAO is the essential role of the conserved residues in maintaining productive conformations for the TPQ cofactor during catalytic turnover. For example, in addition to catalyzing proton abstraction from substrate, the active-site base (Asp319 in HPAO) seems to prevent the formation of nonproductive conformations of resting TPQ and several of its catalytic intermediates, presumably through hydrogen-bonding and electrostatic interactions involving Asp319 and the C-5 position of the cofactor (*23*). In a similar manner, the residues flanking TPQ (within the strictly conserved consensus sequence, Asn-TPQ-Asp/Glu) play a role in controlling the TPQ conformation as a result of their presence in a "loop" that fills up the space behind the back face of the mature cofactor (*16*). One curious feature is that the rate of movement of the cofactor into nonproductive conformations appears to be quite variable. In the case of the resting TPQ, aminoquinol, and iminoquinone forms of cofactor, movement may occur fairly rapidly, whereas two examples thus far indicate that rotation of the product Schiff base into a deprotonated, nonproductive conformation is a relatively slow process [E406N (*28*) and N404A (*16*)]. Y305A appears to be an exception in this regard, since the data presented herein, i.e., the short lifetime of the 388 nm absorbing species and the rapid falloff in rate above pH 7 (Figure 5), support a rapid and reversible production of a noncatalytic form of the product Schiff base. The fact that this process is pH-dependent may indicate that the Schiff base itself is being titrated (Scheme 4), although we cannot rule out the ionization of another residue.

In contrast to the accumulation of an inhibitory product Schiff base complex when methylamine is used as substrate, the similarity of the kinetic parameters for Y305A to WT

HPAO using the larger substrate, ethylamine (Table 2), indicates that Tyr305 is not essential to maintain the cofactor in a productive binding mode during catalysis. This is, perhaps, not surprising, since the available crystal structures for CAOs indicate that Tyr305 lies at the bottom of the TPQ cofactor and would be capable of interactions with the C-4 oxygen of TPQ in either a normal or a flipped conformation. However, some explanation is needed for the formation of a noncatalytic product Schiff base complex with methylamine (but not ethylamine) and Y305A. In this manner, Y305A is most similar to E406N, with the *important* exception that the inhibitory product Schiff base forms and breaks down much more slowly with E406N, allowing its isolation and characterization by resonance Raman spectroscopy at high pH (*28*). One explanation for the behavior of Y305A toward methylamine may be an altered hydrogen-bonding pattern linking the active-site base and the region left vacant at position 305; this linkage of Asp319 to Tyr305 may be extremely important in the maintenance of catalytically viable prototropic forms of intermediates of TPQ during turnover. The state of protonation of the Schiff base intermediate in the reduced cofactor would be expected to be more sensitive to an altered active-site structure than complexes involving the oxidized TPQ, since reduction of TPQ leads to the uptake of a proton at the C-4 oxygen (*27*) and, hence, a reduction in the degree of electrostatic stabilization available for the protonated product Schiff base (cf. Scheme 2). According to such a view, the falloff in rate seen with Y305A and methylamine reflects the ionization of the product Schiff base, which is then accompanied by a rapid rotation of the complex into a nonproductive binding mode away from Asp319. In the case of E406N, published inhibition data have implicated the ionization of a separate active-site residue that appears to "gate" a relatively slow isomerization process that leads to the nonproductive conformation of the product Schiff base (*28*).

Kinetic Parameters for Y305A in Relation to WT HPAO: Evidence for a Change in Substrate Specificity. An analysis of pH dependencies and isotope effects for WT HPAO is shown in Figures 3 and 4 for comparison to Y305A as well as other active-site mutants of HPAO. The observation of two pK_a's on k_{cat}/K_m with methylamine as substrate (Figure 3A) is similar to that seen previously with BSAO (*25*). The pH-invariant deuterium isotope effect (Figure 3B) indicates that the C−H bond cleavage step is at least partially rate-determining. The most straightforward interpretation of the observed pK_a values is that they represent the ionization of the active-site base (pK_a = 8.1) and the substrate amine (pK_a = 9.9). As originally observed with BSAO (*25*), the pK_a of the active-site base is substantially reduced (to pK_a = 5.6) once amine has bound to form the E•S complex. From a structural perspective, a high pK_a for the active-site Asp319 can be rationalized by its proximity to the negative charge on the TPQ cofactor, as well as the presence of hydrophobic residues in the region surrounding Asp319. While benzylamine is a poorer substrate than methylamine for HPAO and a more limited data set was collected (Figure 3C,D), the patterns of pH dependencies and isotope effects appear similar between the two substrates.

The pH profile for k_{cat} for WT HPAO with methylamine as substrate also displays two pK_a values (7.9 and 8.8). The absence of a significant isotope effect using deuterated methylamine suggests that the reoxidation of reduced cofactor may be the rate-limiting step. In a recent study of the oxidative half-reaction with BSAO, Su and Klinman (*12*) have found that the reduced cofactor must be deprotonated before reoxidation and ionizes with a pK_a of 7.2. Use of the slower substrate, benzylamine, leads to a significantly greater rate limitation of k_{cat} by the C−H bond cleavage step and, consequently, a completely different pH dependence. The absence of a discernible trend in k_{cat} vs pH with benzylamine very likely indicates the perturbation of the active-site base to a lower pK_a (i.e., one that lies below the experimental pH range), analogous to what has been previously reported for BSAO (*25*).

The behavior of k_{cat}/K_m with Y305A toward either methylamine or ethylamine (Figure 5B) is very similar to WT HPAO, with regard to both the size of the measured parameters and their pH dependencies. The fitted pK_a values with ethylamine as substrate (8.2 and 9.8) are essentially identical to that seen with the WT HPAO. The falloff in k_{cat} with methylamine (but not ethylamine) has already been discussed above in the context of the movement of the product Schiff base complex with the smaller substrate into a nonproductive conformation. As expected for the formation of inhibitory species off the reaction path, this behavior appears in k_{cat}, but not k_{cat}/K_m. Deuterium isotope effects determined at a single pH with methylamine are also almost identical to those seen with the WT HPAO, supporting a (partial) rate limitation of k_{cat}/K_m by C−H bond cleavage and rate limitation of k_{cat} by a separate step (most likely cofactor reoxidation). The first pK_a seen in k_{cat} for ethylamine with Y305A is 7.3, very close to the pK_a of 7.2 ascribed to the reduced cofactor in BSAO (*25*).

The similarity between WT HPAO and Y305A does not hold when benzylamine is used as substrate. One, as yet, unanswered question for CAOs is the origin of substrate specificity. It appears that replacement of Tyr with Ala at position 305 leads to a greatly reduced capacity for benzylamine turnover in the active site. This effect is most dominant on k_{cat}/K_m for dioxygen (cf. a 1000-fold rate reduction), a surprising result given the presumption of a ping-pong mechanism for all CAOs; as mentioned above, this may reflect a strong sensitivity of Y305A to inhibition by substrate benzylamine (or product benzaldehyde). Inspection of Table 2 shows that the use of benzylamine with WT HPAO also gives a small reduction in k_{cat}/K_m for dioxygen. Deletion of the Tyr at position 305 may create a pocket into which the hydrophobic ring of benzylamine (or benzaldehyde) could migrate, impairing the arrangement of active-site residues and dramatically slowing down the reoxidation of reduced cofactor.

Y305 Replacement by Phenylalanine Is Far More Deleterious than Alanine. Table 1 compares the kinetic parameters for mutants at position 305, using either Ala, Cys, or Phe in place of Tyr. Although Phe is generally considered a more conservative replacement for Tyr than Ala, this is clearly not the case for HPAO. In contrast to the very modest effects of Ala at position 305 using aliphatic substrates, incorporation of Phe at this position gives a ca. 500-fold reduction in k_{cat}/K_m and a ca. 120-fold reduction in k_{cat}. The very slow rates of Y305F have precluded detailed kinetic studies of this mutant. However, the available data clearly indicate that the active-site geometry has been seriously compromised when

Phe is placed at position 305. In an earlier study of human aldose reductase, Bohren et al. found that replacement of an active-site Tyr by His or Ser reduced activity by 10^5, while Phe led to complete loss of activity (*30*). A likely explanation for the effect of Phe in the CAOs lies with the very close proximity between the C-4 oxygen of TPQ and the C-4 oxygen of Tyr305 in WT HPAO. It is possible that the incorporation of Phe at position 305 does not leave sufficient space for a water molecule to bind. In the absence of a functional group capable of hydrogen bonding, the network that links the two active sites in the CAOs (cf. Figure 8) could be disrupted. Additionally, the electronic structure of the active-site cofactor may be seriously compromised [cf. Mure and Klinman (*27*)]. As discussed by Su and Klinman (*12*), the reduced form of TPQ is believed to be the carrier of two protons (one from substrate and one from the axial water coordinated to copper) that are ultimately transferred to dioxygen in its reduction to hydrogen peroxide. In the Y305F mutant, a new pathway may have to be created for the movement of protons from the substrate to the oxygen binding site. Future crystallographic studies of this protein may provide a firmer structural basis for the observed kinetic properties. We note that cysteine substitution comes much closer to the behavior of Ala, presumably because of the ability of the Cys mutant to sustain bound water and, hence, an approximation of the original hydrogen-bonding pathway. These results may have some implications for alanine scanning (*31*), where successive residues of a protein are replaced by alanine to determine the role of that residue in the function of the protein. From these results, we suggest that, in selected cases, results obtained by alanine scanning may be misleading and should be interpreted with care.

CONCLUDING COMMENTS

The data presented herein show that a strictly conserved residue in the active site of CAOs is not essential for either cofactor production or enzymatic turnover. We propose that the roles for Tyr305 in HPAO (and by inference other CAOs) include: (i) the preservation of a hydrogen-bonded network for communication between the two halves of the active site involved in substrate oxidation and dioxygen reduction (cf. Figure 8); and (ii) proper positioning of the TPQ precursor for biogenesis and TPQ-derived intermediates during the catalytic cycle (cf. Figures 5 and 6 and Scheme 4).

At the current time, the least well-understood effect of Y305 is in the biogenesis of TPQ from the Tyr precursor. Thus far, only Ala has been placed at this position. This substitution appears to have an effect on the stability of the precursor protein, on the rate of precursor processing, and on the lifetime of intermediates arising during the biogenic process. Of some note, the data obtained thus far indicate that Tyr305 is not essential for biogenesis, ruling out a role for Tyr305 in the stabilization of a radical intermediate at the Tyr (405) which is the precursor to TPQ, as well as a critical role for Tyr305 as a base catalyst in the aromatic substitution reactions that occur at Tyr405. For the future, we plan to examine a range of amino acid substitutions at position 305, in an effort to accumulate and study the various intermediates of the biogenic pathway.

ACKNOWLEDGMENT

We thank Paul Brooks and Steve Brimmer for assistance with the ICP, Gina Chan for technical assistance, Qiaojuan Su for work on the oxidative half-reaction of HPAO, and Amnon Kohen and Wilson Francisco for helpful discussions.

REFERENCES

1. Kurtzman, C. P. (1984) *Antonie van Leeuwenhoek 50*, 209−217.
2. Cai, D., and Klinman, J. P. (1994) *J. Biol. Chem. 269*, 32039−32042.
3. Cai, D., and Klinman, J. P. (1994) *Biochemistry 33*, 7647−7653.
4. Wilce, M. C. J., Dooley, D. M., Freeman, H. C., Guss, J. M., Matsunami, H., McIntire, W. S., Ruggiero, C. E., Tanizawa, K., and Yamaguchi, H. (1997) *Biochemistry 36*, 16116−16133.
5. Matsuzaki, R., Fukui, T., Sato, H., Ozaki, Y., and Tanizawa, K. (1994) *FEBS Lett. 351*, 360−364.
6. Cai, D., Williams, N. K., and Klinman, J. P. (1997) *J. Biol. Chem. 272*, 19277−19281.
7. Nakamura, N., Matsuzaki, R., Choi, Y.-H., Tanizawa, K., and Sanders-Loehr, J. (1996) *J. Biol. Chem. 271*, 4718−4724.
8. Ruggiero, C., Smith, J. A., Tanizawa, K., and Dooley, D. M. (1997) *Biochemistry 36*, 1953−1959.
9. Klinman, J. P., and Mu, D. (1994) *Annu. Rev. Biochem. 63*, 299−344.
10. Turowski, P. N., Mcguirl, M. A., and Dooley, D. M. (1993) *J. Biol. Chem. 268*, 17680−17682.
11. Medda, R., Padiglia, A., Bellelli, A., Sarti, P., Santanche, S., Finazzi-Agro, A., and Floris, G. (1998) *Biochem. J. 332*, 431−437.
12. Su, Q., and Klinman, J. P. (1998) *Biochemistry 37*, 12513−12525.
13. Parsons, M. R., Convery, M. A., Wilmot, C. M., Yadav, K. D. S., Blakeley, V., Corner, A. S., Phillips, S. E. V., McPherson, M. J., and Knowles, P. F. (1995) *Structure 3*, 1171−1184.
14. Kumar, V., Dooley, D. M., Freeman, H. C., Guss, J. M., Harvey, I., McGuirl, M. A., Wilce, M. C. J., and Zubak, V. M. (1996) *Structure 4*, 943−955.
15. Li, R., Klinman, J. P., and Mathews, F. S. (1998) *Structure 6*, 293−307.
16. Schwartz, B., Green, E. L., Sanders-Loehr, J., and Klinman, J. P. (1998) *Biochemistry 37*, 16591−16600.
17. Hartmann, C., and Klinman, J. P. (1991) *Biochemistry 30*, 4605−4611.
18. Deng, W. P., and Nickoloff, J. A. (1992) *Anal. Biochem. 200*, 81.
19. Plastino, J., and Klinman, J. P. (1995) *FEBS Lett. 371*, 276−278.
20. Bruinenberg, P. G., Evers, M., Waterham, H. R., Kuipers, J., Arnberg, A. C., and Ab, G. (1989) *Biochim. Biophys. Acta 1008*, 157−167.
21. Paz, M. A., Fluckiger, R., Boak, A., Kagan, H. M., and Gallop, P. M. (1991) *J. Biol. Chem. 266*, 689−692.
22. Cleland, W. W. (1979) *Methods Enzymol. 63*, 103−138.
23. Plastino, J. (1997) Ph.D. Thesis, University of California, Berkeley.
24. Hevel, J., Sanders-Loehr, J., and Klinman, J. P., unpublished data.
25. Farnum, M., Palcic, M., and Klinman, J. P. (1986) *Biochemistry 25*, 1898−1904.
26. Christensen, J. J., Izatt, R. M., Wrathall, D. P., and Hansen, L. D. (1969) *J. Chem. Soc. A*, 1212−1223.
27. Mure, M., and Klinman, J. P. (1993) *J. Am. Chem. Soc. 115*, 7117−7127.
28. Cai, D., Dove, J., Nakamura, N., Sanders-Loehr, J., and Klinman, J. P. (1997) *Biochemistry 36*, 11472−11478.
29. Williams, N., and Klinman, J. P., in preparation.
30. Bohren, K. M., Grimshaw, C. E., Lai, C.-J., Harrison, D. H., Ringe, D., Petsko, G. A., and Gabbay, K. H. (1994) *Biochemistry 33*, 2021−2032.
31. Cunningham, B. C., and Wells, J. A. (1989) *Science 244*, 1081−1085.

BI982199M